Disability and Rehabilitation: Assistive Technology

ISSN: (Print) (Online) Journal homepage: https://www.tandfonline.com/loi/iidt20

Electromechanical delay during functional electrical stimulation induced cycling is a function of lower limb position

Brendon C. Allen , Kimberly J. Stubbs & Warren E. Dixon

To cite this article: Brendon C. Allen , Kimberly J. Stubbs & Warren E. Dixon (2021): Electromechanical delay during functional electrical stimulation induced cycling is a function of lower limb position, Disability and Rehabilitation: Assistive Technology

To link to this article: https://doi.org/10.1080/17483107.2021.1878295

Published online: 02 Feb 2021.

Submit your article to this journal

View related articles

View Crossmark data

Full Terms & Conditions of access and use can be found at
https://www.tandfonline.com/action/journalInformation?journalCode=iidt20

DISABILITY AND REHABILITATION: ASSISTIVE TECHNOLOGY
https://doi.org/10.1080/17483107.2021.1878295

Taylor & Francis
Taylor & Francis Group

Check for updates

ORIGINAL RESEARCH

Electromechanical delay during functional electrical stimulation induced cycling is a function of lower limb position

Brendon C. Allen, Kimberly J. Stubbs and Warren E. Dixon

Department of Mechanical and Aerospace Engineering, University of Florida, Gainesville, FL, USA

ABSTRACT

Introduction: Functional electrical stimulation (FES) induced cycling has been shown to be an effective rehabilitation for those with lower limb movement disorders. However, a consequence of FES is an electromechanical delay (EMD) existing between the stimulation input and the onset of muscle force. The objective of this study is to determine if the cycle crank angle has an effect on the EMD.
Methods: Experiments were performed on 10 participants, five healthy and five with neurological conditions resulting in movement disorders. A motor fixed the crank arm of a FES-cycle in 10° increments and at each angle stimulation was applied in a random sequence to a combination of the quadriceps femoris and gluteal muscle groups. The EMD was examined by considering the contraction delay (CD) and the residual delay (RD), where the CD (RD) is the time latency between the start (end) of stimulation and the onset (cessation) of torque. Two different measurements were used to examine the CD and RD. Further, two multiple linear regressions were performed on each measurement, one for the left and one for the right muscle groups.
Results: The crank angle was determined to be statistically relevant for both the CD and RD.
Conclusions: Since the crank angle has a significant effect on both the CD and RD, the angle has a significant effect on the EMD. Therefore, future efforts should consider the importance of the crank angle when modelling or estimating the EMD to improve control designs and ultimately improve rehabilitative treatments.

ARTICLE HISTORY
Received 15 September 2020
Revised 10 January 2021
Accepted 15 January 2021

KEYWORDS
Rehabilitation; functional electrical stimulation; electromechanical delay; contraction delay; residual delay; FES-cycling

➤ IMPLICATIONS FOR REHABILITATION

- New model predicts the delayed response of muscle torque production to electrical stimulation as a function of limb position during FES cycling.
- The model can inform closed-loop electrical stimulation induced rehabilitative cycling.

Introduction

A common rehabilitative exercise for individuals with neurological conditions (NCs) is functional electrical stimulation (FES) induced cycling [1–7], which has been shown to impart numerous health benefits [8–10]. FES applies an electrical stimulus to elicit muscle contractions; however, this complex electro-physiological energy conversion process results in a time latency (i.e., an electromechanical delay (EMD)) between the application of the electrical input and the corresponding muscle contraction [11–14].

The EMD presents a challenge for closed-loop control of a FES system since the EMD can destabilize a control system. Therefore, delay-compensation methods have been investigated in recent years for FES systems [3–6,15–19]. An improved understanding of the EMD can allow for improved closed-loop control designs or estimates of the EMD; however, the EMD has previously only been investigated during coordinated tasks (i.e., FES-cycling) in Allen et al. [14], where the effect of fatigue on the EMD during FES-cycling was characterized.

The objective of this study is to determine if lower limb position, as measured by the crank angle, has an effect on the EMD and to model the EMD as a function of the crank angle. Two types of EMD are considered: the contraction delay (CD) and residual delay (RD), where the CD (RD) is the time latency between the start (end) of stimulation and the onset (cessation) of torque. Experiments were performed on 10 participants, five with NCs resulting in movement disorders, and entailed the motor fixing the crank at pre-set angles and stimulation being applied to a combination of the quadriceps femoris and gluteal muscle groups. Multiple linear regressions were performed to conclude that the crank angle has a significant effect on the EMD.

Materials and methods

Subjects

Ten participants with the demographics shown in Table 1 participated in this study. Participants with a NC are referred to by the letter "N" followed by a participant number and participants without NCs are referred to by the letter "S" followed by a participant number. Each participant provided written informed consent prior to participation, as approved by the University of Florida Institutional Review Board (IRB201901676).

CONTACT Brendon C. Allen brendoncallen@ufl.edu Department of Mechanical and Aerospace Engineering, University of Florida, Gainesville, FL, USA
© 2021 Informa UK Limited, trading as Taylor & Francis Group

Table 1. Participant demographics.

Participant	Age	Sex	Condition	Time since diagnosis
S1	27	M	None	–
S2	28	M	None	–
S3	22	F	None	–
S4	21	M	None	–
S5	23	M	None	–
N1	26	M	Spina bifida (L5-S1)	26 years
N2	57	F	Multiple sclerosis	10 years
N3	42	F	Cerebral palsy	42 years
N4	34	F	Multiple sclerosis	5 years
N5	64	F	Multiple sclerosis	23 years

Apparatus

The modified recumbent tricycle detailed in Cousin et al. [7] was used as the experimental testbed in this study.

Experimental protocol

Electrodes were placed lateral-proximal and medial-distal over the quadriceps femoris muscle group and distal and proximal over the gluteal muscle group. The participant was seated in the cycle and their legs were constrained using orthotic boots. A comfort limit on the pulse width for each muscle group was determined by using the motor to fix the crank at pre-set angles, creating isometric conditions, and then applying transcutaneous electrical stimulation. Throughout the experiments, the stimulation frequency (60 Hz) and current amplitude (70 mA for the gluteals and 90 mA for the quadriceps) were fixed[1] and the pulse width for a given muscle was set to the participant's comfort threshold for the particular muscle. In prior studies, often the gluteal muscle is stimulated only when the quadriceps is being stimulated [2,7,14]; therefore, two muscle combinations are considered: quadriceps only, and quadriceps and gluteal together.

During the experiment, the motor fixed the crank arm in 10° increments (from 10° to 350°) while 0.25 s of stimulation was provided at each angle in a random sequence to the right quadriceps (RQ), left quadriceps (LQ), right quadriceps and gluteal (RQRG) and left quadriceps and gluteal (LQLG) muscle groups. The pulse width input and resulting output torque were recorded with a 500 Hz sampling frequency. Two second rest periods were provided between each application of 0.25 s of stimulation.

Measurements

Before making any measurements, the torque data were forward and reverse filtered, to reduce noise without introducing a delay, using a 2nd order Butterworth IIR low-pass filter with a half power frequency of 8 Hz. The torque and pulse width data were separated into segments that each contained 0.25 s of stimulation and the corresponding torque response. The torque response had three distinct regions within each segment: a pre-contraction region, a muscle contraction region and a post-contraction region. To remove the passive inertial effects that result from the weight of the leg pushing on the torque sensor, the torque data within each segment were shifted to set the average torque of the pre-contraction region to 0.

During FES-cycling, generally stimulation is only applied when the resulting muscle contraction yields efficient forward pedalling of the cycle. Therefore, it was desired to only consider the data that resulted in efficient forward pedalling, which was accomplished by measuring the peak ($T_{\max}$) and average (T_{avg}) torques. Define $T_{\max}$ (T_{avg}) as the maximum (average) value of the torque that results from 0.25 s of stimulation. Torque measurements were converted into a percent, for a given participant and muscle combination, by dividing each $T_{\max}$ (T_{avg}) measurement by the maximum $T_{\max}$ measurement over the entire experiment and multiplying by 100. The percent torques were then plotted, and a subset of angles over which it is efficient (i.e., the median $T_{\max} \geq 40\%$ for both muscle combinations) to stimulate the left and right muscle groups was determined, and the data associated with non-efficient stimulation were removed (e.g., all data associated with stimulation of a given muscle group at a non-efficient angle for that muscle group). Two CD and two RD measurements were made using the remaining data. Define CD25 (CD75) as the difference in time between the instant stimulation began and the instant the torque increased to 25% (75%) of $T_{\max}$ and define RD25 (RD75) as the difference in time between the instant stimulation ended and the instant the torque fell to 25% (75%) of $T_{\max} - \bar{\mu}$, where $\bar{\mu}$ is the average value of the post-contraction region.

Statistical analysis

A multiple linear regression was performed separately on the CD25, CD75, RD25 and RD75 measurements to characterize the effect of the crank angle on the EMD. However, since the left and right muscle groups are effective over different sets of angles (e.g., 50° to 160° for the right muscle groups and 230° to 340° for the left muscle groups), two regressions were performed for each measurement: one for the left muscle groups and another for the right. To allow for a comparison between the left and right muscle groups, the angle was shifted before performing a regression. For the right (left) angle data, the angle was subtracted by 50 (230). The regressions used the following predictors: crank angle (angle; quantitative predictor ranging from 0 to 110 for both muscle groups due to shifting the data), the muscle combination (side; RQ or RQRG for the right muscle groups and LQ or LQLG for the left muscle groups), the individual being tested (subject; N1, … , N5, S1, … , S5), and the quadratic term Angle^2. The reference levels for the categorical predictors were selected as N1 for subject and RQ (LQ) for the right (left) muscle groups. Thus, the subsequent regressions do not include a coefficient for N1, RQ or LQ since their effects are included in the constant term of the regression table.

Interpretation

To determine if the crank angle (and hence lower limb position) has a significant effect on the EMD, the statistical significance of the Angle and Angle^2 predictor coefficients was used. The coefficients for categorical predictors represent vertical shifts, while the coefficients for quantitative predictors represent slopes. The regression over the right (left) muscle groups provides a result that is effective over the crank angles 50° to 160° (230° to 340)°. However, recall that the angles were shifted prior to performing the regressions. Therefore, as an example, the CD25 regression for the right muscle groups, for a given subject and side, would yield a model with the following form:

$$\text{CD25}(q) = A + B(q - 50) + C(q - 50)^2, q \in [50, 160], \qquad (1)$$

where the coefficients A, B and C are scalars obtained from the CD25 regression table for the right muscle groups.

Results

Plots of the percent torques are depicted in Figure 1 and plots of the EMD measurements are shown in Figures 2 and 3. Regressions were performed on each EMD measurement for both the left and right muscle groups using the data depicted in Figures 2 and 3, and the results are included in Tables 2–9. For

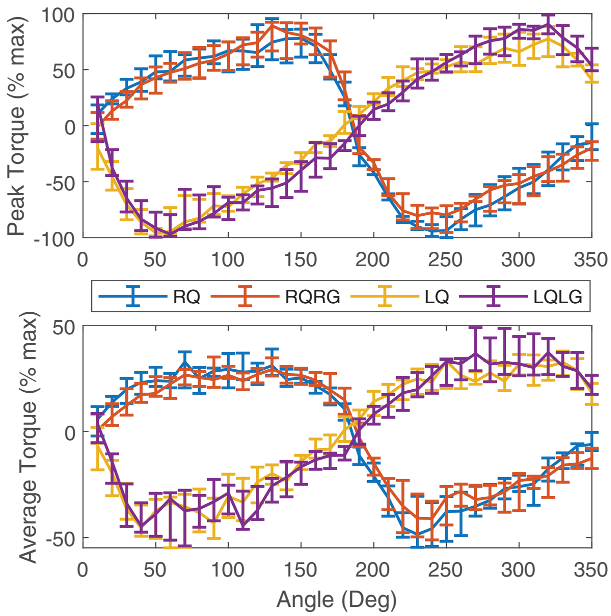

Figure 1. Torque measurements for each muscle combination (i.e., right quadriceps (RQ), right quadriceps and gluteal (RQRG), left quadriceps (LQ) and left quadriceps and gluteal (LQLG) muscle groups). The values show the median across all subjects and the lower and upper error bar denote the 25th (Q1) and 75th (Q3) percentiles, respectively. For a given muscle combination and participant, the peak (average) torque was converted into a percent by dividing each peak (average) torque measurement by the maximum peak torque measurement for the same participant and muscle combination over the entire experiment and multiplying by 100. The 0° crank angle corresponds to the crank being horizontal with the ground and the right leg extended. Consistent with the findings in Bellman et al. [2], the peak and average torques vary in a sinusoidal manner with the crank angle. The torque measurements show that at some angles there is negligible torque production, known as kinematic deadzones [2,7,20], and other angles are more efficient for positive torque production.

visual clarity, non-significant (p values $>$ .05) regression coefficients in each table are denoted by ns, and statistical significance is indicated by *, ** and *** for p values less than or equal to .05, .01 and .001, respectively. Each regression model was validated by generating normal probability plots of the residual errors and visually confirming normality. Additionally, the adjusted R^2 was between 67% and 76% (47% and 68%) for each CD (RD) regression, indicating a good fit [12]. Angle and/or Angle^2 were statistically significant predictors (p value$<$.05) for each CD and RD regression, indicating the crank angle has a significant effect on both the CD and the RD, and hence the EMD.

A couple of examples are presented to demonstrate the model provided by the regression tables. The form of the model for the CD25 regression for the right muscle groups is included in (1), where coefficient A is obtained by adding the constant, subject and side coefficients from Table 2 as applicable. Note that the subject and side coefficients are associated with a specific participant or muscle combination and recall that Tables 2–9 do not include a coefficient for N1, RQ or LQ since their effects are included in the constant terms of the regression tables. Furthermore, coefficients B and C are obtained from the Angle and Angle^2 coefficients in Table 2, respectively. For example, the model of CD25 for participant S1 and the RQ muscle is $CD25(q) = 84.94 - 0.29(q-50) + 0.0054(q-50)^2, q \in [50, 160]$. Likewise, using Table 6, the model of CD25 for participant S1 and the LQ muscle is $CD25(q) = 92.27 - 0.12(q-230) + 0.0033(q-230)^2, q \in [230, 340]$.

Discussion

Participants with and without NCs were recruited in this study. Interestingly, both populations displayed similar trends, and hence, the data for all participants were combined when

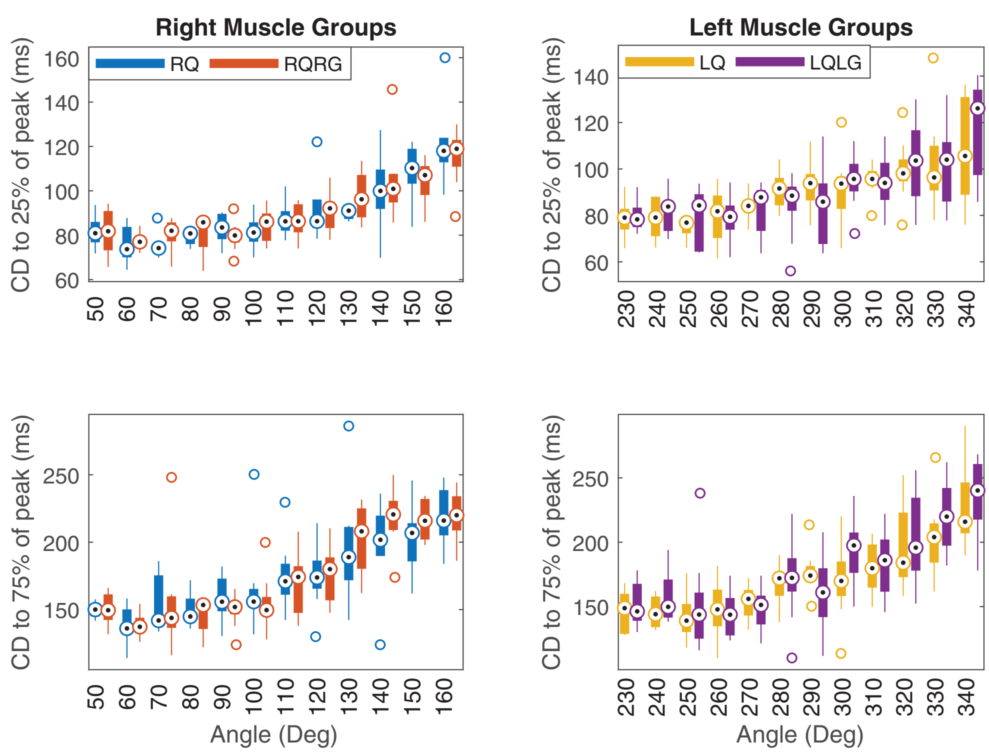

Figure 2. Box plots of the contraction delay (CD) measurements for each muscle combination (i.e., right quadriceps (RQ), right quadriceps and gluteal (RQRG), left quadriceps (LQ) and left quadriceps and gluteal (LQLG) muscle groups). The black dot within a white circle denotes the median, and the box edges denote the 25th (Q1) and 75th (Q3) percentiles. The most extreme, non-outlier, data points are indicated by the whiskers and the outliers are indicated by circles. An outlier is a point above Q3 + 1.5(Q3–Q1) or below Q1–1.5(Q3–Q1). The 0° crank angle corresponds to the crank being horizontal with the ground and the right leg extended. In each subplot, the CD appears to initially be relatively flat and to then increase with the crank angle. In Muraoka et al., the delay was measured at multiple joint angles and it was determined that the delay is dependent on the joint angle until the tendon slack is taken up, at which point the delay becomes constant for further joint angle changes [21]. Therefore, it is possible that the crank angles where the CD was relatively constant correspond to the crank angles where the tendon slack is taken up.

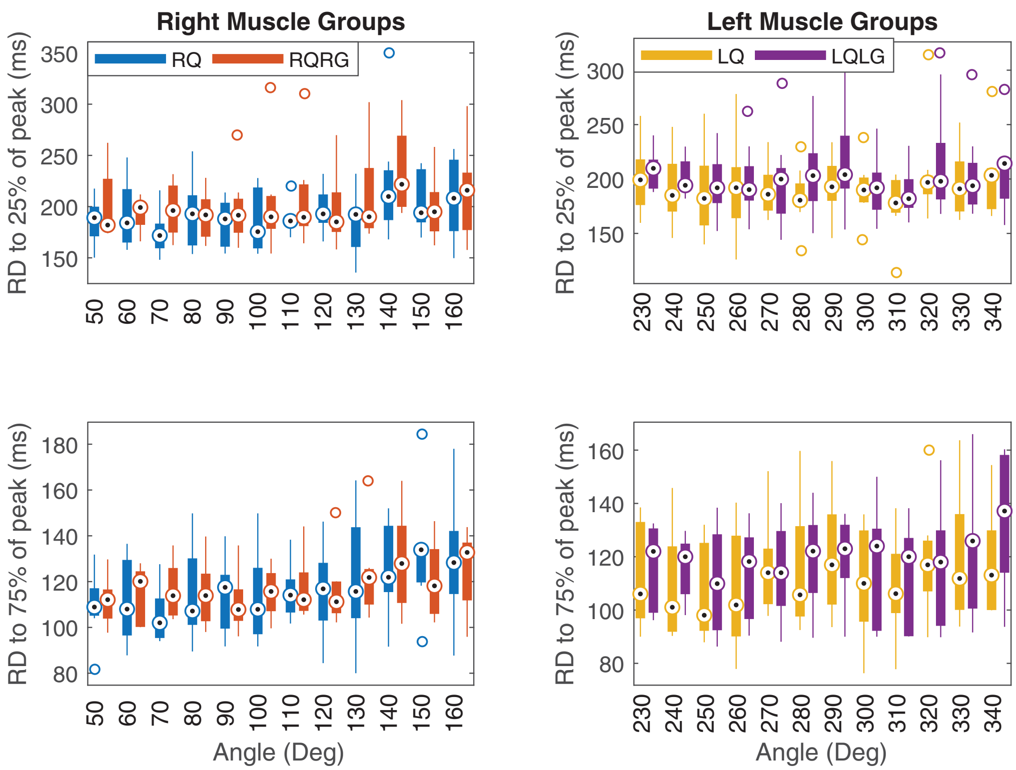

Figure 3. Box plots of the residual delay (RD) measurements for each muscle combination (i.e., right quadriceps (RQ), right quadriceps and gluteal (RQRG), left quadriceps (LQ) and left quadriceps and gluteal (LQLG) muscle groups). The black dot within a white circle denotes the median, and the box edges denote the 25th (Q1) and 75th (Q3) percentiles. The most extreme, non-outlier, data points are indicated by the whiskers and the outliers are indicated by circles. An outlier is a point above Q3 + 1.5(Q3–Q1) or below Q1–1.5(Q3–Q1). The 0° crank angle corresponds to the crank being horizontal with the ground and the right leg extended. By visual inspection of the RD subplots, the effect of the angle on the RD appears to be unclear.

Table 2. Regression on CD25 for the right muscle groups, where the angle coefficients are multiplied by $(q-50) \in [0, 110]$, where q is the crank angle.

	CD25			
Term	Coef.	SE coef.	p Value	Sig.
Constant	85.06	2.69	.000	***
Angle	−0.29	0.07	.000	***
Angle^2	0.0054	0.0006	.000	***
Side				
RQRG	0.76	1.20	.528	ns
Subject				
N2	−1.12	2.65	.674	ns
N3	−13.58	4.31	.002	**
N4	−4.04	2.52	.110	ns
N5	−7.57	3.03	.013	*
S1	−0.12	2.84	.967	ns
S2	5.42	2.49	.031	*
S3	0.65	2.53	.799	ns
S4	−12.24	2.51	.000	***
S5	−3.02	2.61	.250	ns
R^2 adj	73.1%			

Table 3. Regression on CD75 for the right muscle groups where the angle coefficients are multiplied by $(q-50) \in [0, 110]$, where q is the crank angle.

	CD75			
Term	Coef.	SE coef.	p Value	Sig.
Constant	164.34	6.73	.000	***
Angle	−0.12	0.18	.507	ns
Angle^2	0.0073	0.0015	.000	***
Side				
RQRG	0.38	3.01	.899	ns
Subject				
N2	−1.03	6.61	.877	ns
N3	−33.71	10.76	.002	**
N4	−10.68	6.29	.091	ns
N5	−24.98	7.56	.001	***
S1	−22.37	7.08	.002	**
S2	−10.30	6.23	.100	ns
S3	−4.12	6.32	.515	ns
S4	−40.55	6.27	.000	***
S5	−11.93	6.53	.069	ns
R^2 adj	67.5%			

generating the plots and performing the regressions. Similarly, in Allen et al., it was observed that although variability may exist between participants with and without NCs, the overall trends were consistent across the different populations [14].

By inspection of Figures 2 and 3, the CD and RD appear to behave differently. This is consistent with the findings in Allen et al. [14], where it was concluded that the CD and the RD are different. The crank angle appears to have a smaller, although still significant, effect on the RD compared to the CD. Furthermore, from the regression results in Tables 2–9, it was determined that the crank angle and the muscle combination have a significant effect on the EMD during FES-cycling. Since the lower limb position is a function of the crank angle, it could be concluded that the EMD is a function of the lower limb position during FES-cycling.

The results in this work could lead to an improved dynamic model of the FES-cycle system, which could result in improved closed-loop FES control. For example, the dynamic model should allow for the EMD to be different for each muscle combination, the CD, and the RD. Furthermore, when developing an estimator of the EMD, it should allow for the EMD to be a function of the crank angle. Additionally, closed-loop controllers often use bounds on the EMD to account for inter-subject variability and to determine when stimulation should or should not be applied to

Table 4. Regression on RD25 for the right muscle groups, where the angle coefficients are multiplied by $(q-50) \in [0, 110]$, where q is the crank angle.

	RD25			
Term	Coef.	SE coef.	p Value	Sig.
Constant	171.02	6.83	.000	***
Angle	−0.26	0.18	.141	ns
Angle^2	0.0041	0.0015	.008	**
Side				
RQRG	6.39	3.05	.038	*
Subject				
N2	28.42	6.72	.000	***
N3	16.42	10.92	.134	ns
N4	47.27	6.38	.000	***
N5	31.56	7.67	.000	***
S1	−17.39	7.19	.017	*
S2	12.31	6.32	.053	ns
S3	7.92	6.41	.218	ns
S4	6.27	6.36	.325	ns
S5	44.05	6.62	.000	***
R^2 adj	49.9%			

Table 5. Regression on RD75 for the right muscle groups, where the angle coefficients are multiplied by $(q-50) \in [0, 110]$, where q is the crank angle.

	RD75			
Term	Coef.	SE coef.	p Value	Sig.
Constant	102.40	4.39	.000	***
Angle	−0.05	0.11	.653	ns
Angle^2	0.0020	0.0010	.043	*
Side				
RQRG	0.61	1.96	.754	ns
Subject				
N2	18.50	4.32	.000	***
N3	6.83	7.02	.332	ns
N4	33.60	4.11	.000	***
N5	14.08	4.93	.005	**
S1	−7.95	4.62	.087	ns
S2	6.53	4.07	.110	ns
S3	1.75	4.13	.673	ns
S4	4.18	4.09	.309	ns
S5	8.62	4.26	.045	*
R^2 adj	47.1%			

Table 6. Regression on CD25 for the left muscle groups, where the angle coefficients are multiplied by $(q-230) \in [0, 110]$, where q is the crank angle.

	CD25			
Term	Coef.	SE coef.	p Value	Sig.
Constant	67.33	2.29	.000	***
Angle	−0.12	0.07	.092	ns
Angle^2	0.0033	0.0006	.000	***
Side				
LQLG	0.56	1.18	.643	ns
Subject				
N2	21.98	2.53	.000	***
N3	−0.59	3.04	.846	ns
N4	18.72	2.37	.000	***
N5	20.61	2.45	.000	***
S1	24.94	2.61	.000	***
S2	12.51	2.48	.000	***
S3	2.40	2.42	.3237	ns
S4	35.59	2.79	.000	***
S5	15.05	2.39	.000	***
R^2 adj	75.3%			

Table 7. Regression on CD75 for the left muscle groups, where the angle coefficients are multiplied by $(q-230) \in [0, 110]$, where q is the crank angle.

	CD75			
Term	Coef.	SE coef.	p Value	Sig.
Constant	134.66	5.56	.000	***
Angle	−0.29	0.165	.083	ns
Angle^2	0.0084	0.0014	.000	***
Side				
LQLG	5.80	2.85	.043	*
Subject				
N2	23.29	6.15	.000	***
N3	−9.18	7.37	.214	ns
N4	15.16	5.74	.009	**
N5	26.25	5.95	.000	***
S1	27.21	6.34	.000	***
S2	25.67	6.02	.000	***
S3	2.19	5.88	.710	ns
S4	58.28	6.76	.000	***
S5	7.05	5.81	.227	ns
R^2 adj	68.9%			

Table 8. Regression on RD25 for the left muscle groups, where the angle coefficients are multiplied by $(q-230) \in [0, 110]$, where q is the crank angle.

	RD25			
Term	Coef.	SE coef.	p Value	Sig.
Constant	175.69	6.59	.000	***
Angle	−0.39	0.196	.048	*
Angle^2	0.0044	0.0017	.009	**
Side				
LQLG	7.54	3.38	.027	*
Subject				
N2	49.10	7.29	.000	***
N3	84.37	8.73	.000	***
N4	28.70	6.81	.000	***
N5	26.85	7.06	.000	***
S1	12.66	7.52	.094	ns
S2	10.46	7.14	.145	ns
S3	−16.34	6.97	.020	*
S4	53.23	8.02	.000	***
S5	8.23	6.89	.234	ns
R^2 adj	54.3%			

Table 9. Regression on RD75 for the left muscle groups, where the angle coefficients are multiplied by $(q-230) \in [0, 110]$, where q is the crank angle.

	RD75			
Term	Coef.	SE coef.	p Value	Sig.
Constant	94.22	3.13	.000	***
Angle	−0.16	0.09	.078	ns
Angle^2	0.0022	0.0008	.007	**
Side				
LQLG	2.51	1.61	.120	ns
Subject				
N2	42.17	3.47	.000	***
N3	39.29	4.15	.000	***
N4	31.75	3.24	.000	***
N5	28.22	3.35	.000	***
S1	16.28	3.57	.000	***
S2	5.63	3.39	.099	ns
S3	−2.38	3.31	.474	ns
S4	40.42	3.81	.000	***
S5	14.75	3.27	.000	***
R^2 adj	67.8%			

yield muscle contractions in regions of the crank cycle that result in efficient forward pedalling of the cycle [3–6]. Tables 2–9 could be used to establish bounds on the EMD across a range of participants at each crank angle or across all crank angles to further enable the development of closed-loop FES-cycling controllers. Although the EMD measurements in Tables 2–9 could vary if different stimulation patterns were provided or if the cycle seat was adjusted differently (future studies would be required to determine the exact effect of these variations), the largest variation in the EMD is likely between subjects, which motivated including data from a range of participants in Tables 2–9.

In conclusion, the regression results in Tables 2–9 establish models of the EMD as a function of the cycle crank angle. Further, it was concluded that the EMD during FES-cycling is a function of lower limb position. The finding that the EMD is a function of the lower limb position is true, in general, and is agnostic to the specific exercise being performed. However, different exercises may result in a different combination of muscle groups being active at a given time, which would impact the model. Future studies would be required to establish specific models of the EMD for these other activities. The conclusions of this paper provide EMD and dynamic model insights, which could lead to improved closed-loop FES controllers or improved estimators of the EMD that ultimately may improve rehabilitative treatments.

Note

1. The selection of the amplitudes and frequency were based on prior literature [2].

Disclosure statement

No potential conflict of interest was reported by the author(s).

Funding

This research is supported in part by NSF Award number 1762829 and the National Defense Science and Engineering Graduate Fellowship Program.

ORCID

Brendon C. Allen http://orcid.org/0000-0002-5994-0932

References

[1] Petrofsky JS. New algorithm to control a cycle ergometer using electrical stimulation. Med Biol Eng Comput. 2003;41(1):18–27.

[2] Bellman MJ, Downey RJ, Parikh A, et al. Automatic control of cycling induced by functional electrical stimulation with electric motor assistance. IEEE Trans Automat Sci Eng. 2017;14(2):1225–1234.

[3] Allen BC, Cousin C, Rouse C, et al. Cadence tracking for switched FES cycling with unknown input delay. Proceedings of the IEEE Conference on Decision and Control; 2019.

[4] Allen B, Cousin C, Rouse C, et al. Cadence tracking for switched FES-cycling with unknown time-varying input delay. Proceedings of the ASME Dynamic Systems & Control Conference; 2019.

[5] Allen BC, Stubbs K, Dixon WE. Robust cadence tracking for switched FES-cycling with an unknown time-varying input delay using a time-varying estimate. IFAC World Congress; 2020.

[6] Allen BC, Stubbs K, Dixon WE. Robust power and cadence tracking on a motorized FES cycle with an unknown time-varying input delay. Proceedings of the IEEE Conference on Decision and Control; 2020.

[7] Cousin CA, Rouse CA, Duenas VH, et al. Controlling the cadence and admittance of a functional electrical stimulation cycle. IEEE Trans Neural Syst Rehabil Eng. 2019;27(6):1181–1192.

[8] Mohr T, Pødenphant J, Biering-Sørensen F, et al. Increased bone mineral density after prolonged electrically induced cycle training of paralyzed limbs in spinal cord injured man. Calcif Tissue Int. 1997;61(1):22–25.

[9] Hooker SP, Figoni SF, Rodgers MM, et al. Physiologic effects of electrical stimulation leg cycle exercise training in spinal cord injured persons. Arch Phys Med Rehabil. 1992;73(5):470–476.

[10] Ferrante S, Pedrocchi A, Ferrigno G, et al. Cycling induced by functional electrical stimulation improves the muscular strength and the motor control of individuals with post-acute stroke. Eur J Phys Rehabil Med. 2008;44(2):159–167.

[11] Cè E, Rampichini S, Agnello L, et al. Effects of temperature and fatigue on the electromechanical delay components. Muscle Nerve. 2013;47(4):566–576.

[12] Downey R, Merad M, Gonzalez E, et al. The time-varying nature of electromechanical delay and muscle control effectiveness in response to stimulation-induced fatigue. IEEE Trans Neural Syst Rehabil Eng. 2017;25(9):1397–1408.

[13] Ha KH, Murray SA, Goldfarb M. An approach for the cooperative control of FES with a powered exoskeleton during level walking for persons with paraplegia. IEEE Trans Neural Syst Rehabil Eng. 2016;24(4):455–466.

[14] Allen BC, Stubbs KJ, Dixon WE. Characterization of the time-varying nature of electromechanical delay during FES-cycling. IEEE Trans Neural Syst Rehabil Eng. 2020;28(10):2236–2245.

[15] Obuz S, Downey RJ, Klotz JR, et al. Unknown time-varying input delay compensation for neuromuscular electrical stimulation. IEEE Multi-Conference on Systems and Control; 2015. p. 365–370.

[16] Obuz S, Downey RJ, Parikh A, et al. Compensating for uncertain time-varying delayed muscle response in isometric neuromuscular electrical stimulation control. Proceedings of the American Control Conference; 2016. p. 4368–4372.

[17] Sharma N, Gregory C, Dixon WE. Predictor-based compensation for electromechanical delay during neuromuscular electrical stimulation. IEEE Trans Neural Syst Rehabil Eng. 2011;19(6):601–611.

[18] Alibeji N, Kirsch N, Farrokhi S, et al. Further results on predictor-based control of neuromuscular electrical stimulation. IEEE Trans Neural Syst Rehabil Eng. 2015;23(6):1095–1105.

[19] Karafyllis I, Malisoff M, de Queiroz M, et al. Predictor-based tracking for neuromuscular electrical stimulation. Int J Robust Nonlinear Control. 2015;25(14):2391–2419.

[20] Sharma N, Kirsch NA, Alibeji NA, et al. A nonlinear control method to compensate for muscle fatigue during neuromuscular electrical stimulation. Front Robot AI. 2017;4:68.

[21] Muraoka T, Muramatsu T, Fukunaga T, et al. Influence of tendon slack on electromechanical delay in the human medial gastrocnemius in vivo. J Appl Physiol (1985). 2004;96(2):540–544.